

## Influence of Tool Geometry on the Quality and Mechanical Properties of FSW Weldment for Al-alloy (7020-T53)

Muhsin Jaber Jweeg\*

Moneer Hameed Tolephih \*\*

Muhammed Abdul-Sattar\*\*\*

\*Alnahrain University - College of Engineering

\*\* Foundation of technical education Technical College – Baghdad

\*\*\*Alnahrain University - College of Engineerin  
[m1976sjn@yahoo.com](mailto:m1976sjn@yahoo.com)\*\*\*

### Abstract:

In this paper the influence of tool geometry and welding parameters (rotating speed and travel speed) on the quality and mechanical properties by using friction stir welded joints for (7020-T53) aluminum alloy.

Three types of tool geometry variables were used ( pin, shoulder and shoulder inclination), internal defect (tunnel) was detected by using X-Ray radiography for all samples which are welded at welding parameters (rotating speed and travel speed), perfect tool geometry that gives defect free was by increasing pin diameter with threaded ,increasing shoulder diameter and shoulder inclination ( $2^{\circ}$ ) for safety purpose radiography test was also performed to examine defect free of weldments (increasing tool dimensions and pin threaded gives increasing stir and heat input).

The effect of welding parameters (rotation and travel speed) using tool geometry that gives defect free were investigated using different mechanical tests including (tensile, bending and microhardness). Macro and microstructure change during (FSW) process were studied and different welding zones were investigated using optical microscope. Based on the friction stir welding experiments conducted in this study the result show that aluminum

alloy (7020-T53) can be welded using FSW process, the optimum welding parameters 1400rpm rotational tool speed and 40mm/min travel speed which give the maximum welding efficiency (83%), increasing rotational speed the microhardness increases in weld zone due to decreasing the grain size.

**Keywords:** Friction stir welding, Mechanical properties and Microstructure and 7020-T53 aluminum alloy.

### Introduction

Friction stir welding (FSW) is a relatively new solid-state welding process invented by The Welding Institute in 1991[1]. FSW is becoming an important joining process because it makes high-quality welds for number of materials. FSW has several advantages, such as low energy input, short welding time, low welding temperatures, and relatively low distortion as compared to the conventional welding methods [1]. The most effective parameters on properties of friction stir welds as well as realizing their influence on the weld properties has been major topics of interest for researchers. The effect of some important parameters such as axial force, rotational speed, and traverse speed on weld properties have been investigated [2].

A schematic representation of the FSW tool and technique is shown in Fig. (1), where a nonconsumable welding tool is used. The tool consists of a cylindrical shoulder with specially profiled projected pin. FSW tool rotates in the speed of several hundred revolutions per minute (rpm). Such rotating tool slowly plunges into the joint line until the shoulder of the welding tool contacts the surface of the plates which are to be joined [1]. Sufficient dwell time is allowed in order to generate frictional heat. It allows the tool to move along the joint line. As a result, the plasticized material is transformed from the leading edge of the tool to the rear side. Ultimately, it produces a high-quality joint between the two plates by the translation movement of the work piece along with applied pressure of the tool.

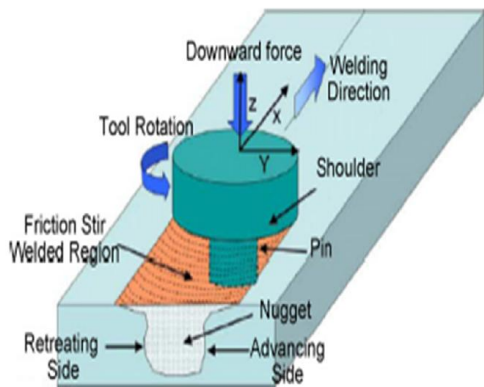


**Figure (1) A comprehensive sketch outlining the friction stir welding technique [1]**

In FSW, the process parameters have to be determined separately for each new component and alloy. The welding speed depends on several factors, such as alloy type, rotational speed, penetration depth, and joint type [3]. In the process, FSW generates several microstructurally distinct regions such as the weld nugget or stir zone, thermomechanically

affected zone, and heat-affected zone [4]. The parameters of the thermomechanical cycle, i.e. total strain, strain rate, and temperature, also control the microstructural. Kumar K, Satish V. Kailas [5] have been investigated the influence of axial load and the of position of the interface with respect to the tool axis on tensile strength of the friction stir welded joint has been investigated the axial load is continuously varied by linearly increasing the interference between the tool shoulder and the surface of the base material the base material used is Al-Zn-Mg alloy, 7020-T6, it is found that there is an optimal axial load above which the weld is defect free.

Gaafer A.M., Mahmoud T.S., Mansour E.H [6] studied the mechanical and microstructural characteristics of friction stir welded AA7020-0 Aluminum plate were investigated. The influence of the tool rotational and welding speeds such characteristics was studied the friction stir welding (FSW) was conducted at the tool rotation speed of 1120, 1400 and 1800rpm at welding speeds of 20, 40 and 80mm/min .it has been found that increasing the tool rotational speed and/or reducing welding speed increases the primary Al phase grain size as well as the size of the precipitates at the center of the stirred zone (SZ). The tensile characteristics of the friction stir welded tensile samples depend significantly on both the tool rotational and welding speeds. Christian B. Fuller Z.W.Chen [7] studied material flow with a closer focus on observation the resulting weld pattern adjacent to the tool pin. An alternative experimental technique was used to freeze the tool pin. This was done by naturally breaking the pin during FSW and hence the tool pin can be embedded in the work piece.

Samples of broken pins and surrounding work piece material after FSW where then made for metallurgical observation. After analyzing the structure features, material flow adjacent to the tool pin is suggested under the steady state FSW condition of 5085-0 a portion of the shear zone material adjacent to the pin formed a layer and detached from the pin on the trailing retreating side during each revolution the detached layers thus formed the nugget zone.

M. Awing2011[8]. He was studied the effect of heat treatment to the material could increase the tensile strength of friction stir welding welds, heat treatable aluminum alloy such as 2, 6 or 7 xxx series are preferable to give closer tensile strength of welds to the parent metal tensile strength whereas the tunnel defect occurred in the weld, can be avoided by choosing suitable welding process parameter s for aluminum alloy such as rotational speed transverse speed or stirring time during the plunging. In the present investigation, examine the welding joints by using X-Ray Radiography to detect defects for three types of tool, mechanical properties and microstructural aspects with various welding speeds and rotational speeds have been investigated for successful welding process.

**Experimental methods:**

The base material used in this study is aluminum alloy 7020-T53. Table (1) shows the chemical composition. Mechanical properties of the material used in this work (Yield stress (345MPaProof stress 0.2%), Ultimate tensile strength (392MPa) and Elongation EL. (15%).

**Table (1) Chemical composition of the base metal used in wt%**

Si	Fe	Cu	Mn	Mg
0.166	0.256	0.142	0.111	1.29
Ni	Zn	Ti	Be	Pb
0.0037	4.61	0.0424	0.00062	0.0066
V	Zr	Al	Cr	Sn
0.0081	0.140	balance	0.213	≤0.0010

(FSW) trials are carried out on a vertical milling machine with square butt joint configuration. A pair of work pieces of dimensions (150mm\*95mm\*5mm) are butted and clamped rigidly on the backing plate for welding. The tools geometry used for this study is as shown in figure (2). Types of tool:

- a) High speed steel with shoulder diameter (15mm) with chamfered edge inclined angle with (2.5°) and cylindrical pin diameter (5mm) not threaded and pin depth (4.8mm) figure (2-a) .
- b) Material type steel X12M with shoulder diameter (18mm) with chamfered edge inclined angle with 8° and cylindrical pin diameter (6mm) threaded with (M6=1mm pitch) and pin depth (4.8mm) figure (2-b).
- c) Material type steel X12M with shoulder diameter (18mm) with chamfered edge inclined angle with 2° and cylindrical pin diameter (6mm) threaded with (M6=1mm pitch) and pin depth (4.85mm) figure (2-c).

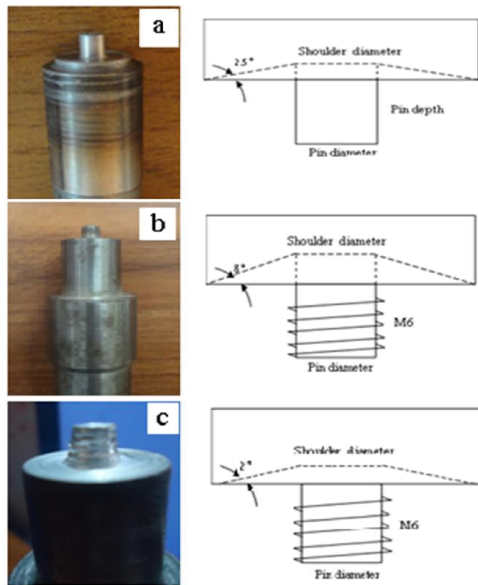


**Figure (2) the tools geometry used for welding process.**

The welds were made on one side using two combinations of tool rotation speed (710rpm, 900rpm, 1120rpm and 1400rpm) and welding travel speed (16mm/min, 25mm/min and 40mm/min).

The microhardness Vickers tests were performed using a 500-g load for 10 s dwell time on the cross section, perpendicular to the welding direction. Tensile test was carried out according to ASTM (B557M) and tested in a perpendicular direction to the welding. Three point bending test was carried out to determine the maximum bending force of the welded joints. The shape and dimensions of the bending specimens according to ASME (QW-462). All tensile and bending tests were carried out at room temperature and constant loading rate (5mm/min) by computerized universal testing machine united HI808. These specimens were polished and etched using Keller's reagent; specimens were examined using optical microscope Nikon microscope.

FSW specimens were prepared from the area which is transverse to the weld direction; a Radiography inspection was also performed using X-Rays at 120kV and 0.4 mA in order to find out identity the internal defects such as tunnel.

## Results and Discussion:

### Weld defects:

The superficial appearance of the welds carried out on the alloy 7020-T53 using all tools type, the different zones: a shoulder flow zone, a nugget zone with a ring/layer structure, and a swirl zone. The thermo mechanically affected zone (TMAZ) outside these three zones fig. (3-b).

A continuous weld defect, indicated by an arrow in the figure (3-a) (1400rpm) (40mm/min) was observed on the advance side, along almost the entire length of the welds. In fact in all welding parameter were selected this defect appear. Defect located at the triple junction of swirl zone, Nugget zone and the outside A transverse cross-section of a weld plate showing the top zone, Nugget zone and the swirl zone. (but lower) TMAZ. The closing of this lower junction void again requires a slightly higher plastic flows that form the swirl and Nugget zones. The weld zones and defects are particularly similar to the welds made using a similar alloy with similar FSW conditions [9]. The presence of these two small void defects has provided a good indication of material flow directions in general as shown in figure (3-b).

The X-Ray inspections for tool (1) in fig. (3-a) show the defects already detected by visual inspection both figures (3-a), (3-b) and (3-c) depict the same weld the X-Ray examination that was done from the face of the weld the presence of the defects on the advancing side was also

checked by macro examination the morphological appearance of the tunnel defects suggests these defects are void origination from the flux path of the material around the pin, M. Awing et. al. 2011[8] and Leal et. al. [9].

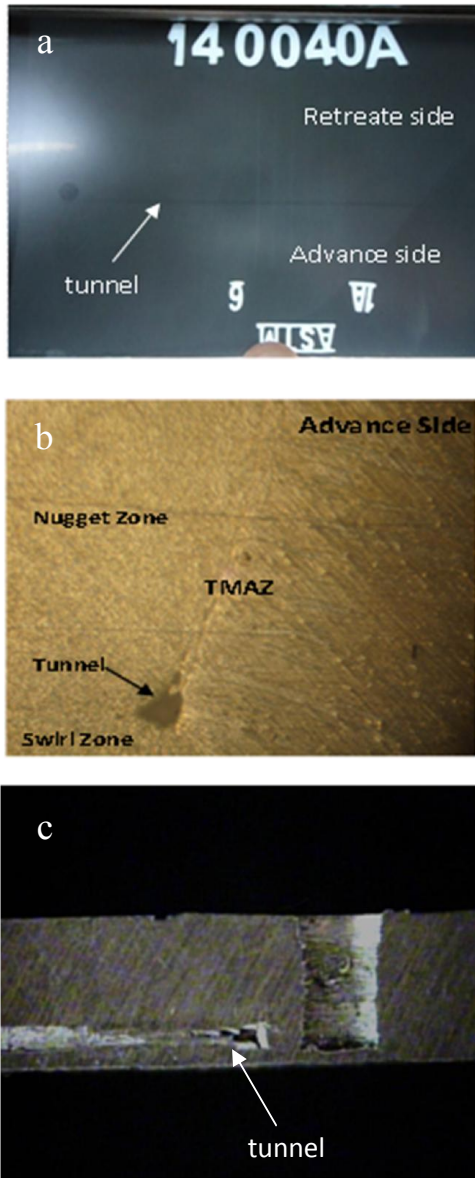


Figure (3) X-Ray radiography and macrograph shows the defect appearance with tool (1) at 1400rpm and 40mm/min

For tool number (2) also a continuous weld defect indicated along weld direction under pin near the root as shown in fig.4 also this defects appear in all welding parameters.

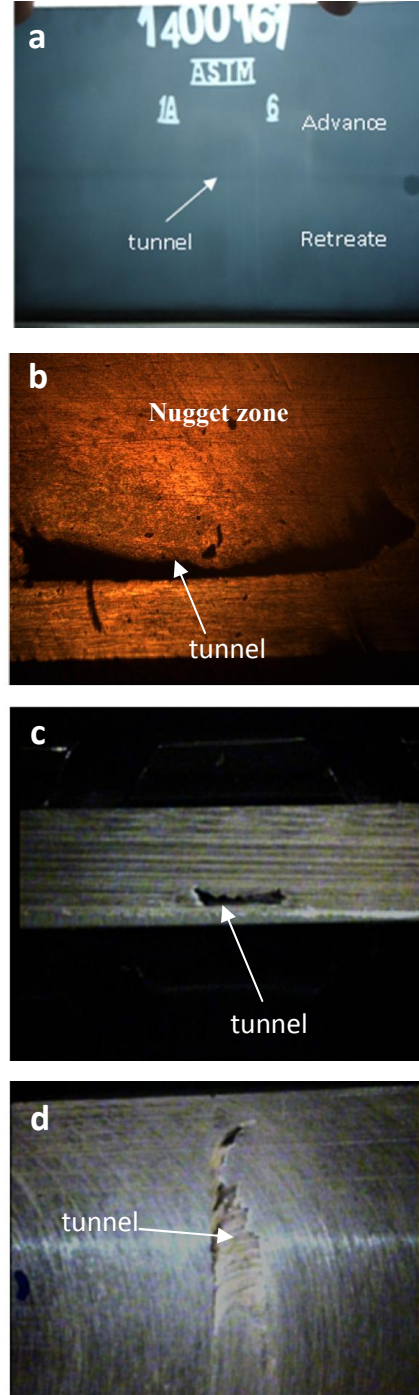
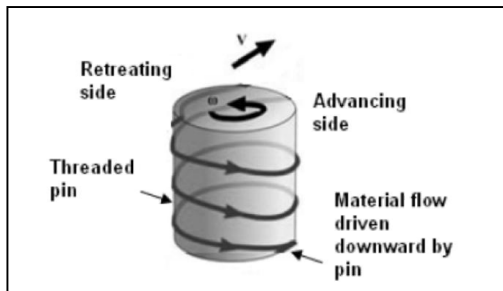


Figure (4) X-Ray radiography and macrograph shows the defects appearance with tool (2)

from tool geometry shoulder diameter (18mm) in tool (2) is higher than tool (1) and the pin is threaded with (M6) but in tool (1) is smooth cylinder and shoulder inclination in tool (2) is (8 degree) while in tool (1) is (2 degree), from that increasing in tool geometry increase in heat input for work piece and threaded cylinder increasing stirring around the pin [11], tool pins are designed to disrupt the contacting surfaces of the workpiece, shear workpiece material in front of tool pin, and move material behind the tool pin, as illustrated in Fig. 5.



**Figure 5: Schematic illustration of threaded pin drives material flow down to the bottom of the pin**

Threads cut on the pin are used to transfer the material flow from the shoulder face down to the bottom of the pin. Fuller, C.B 2007[12], but increasing the inclination in shoulder explained that the primary reason for the defect in the welds for tool (2), at the initial stages, where the inclination of shoulder was less than 2 degree, is shallow shoulder penetration (lack of shoulder contact with the base material). When the depth of shoulder penetration was increased the axial load increased and when the axial load the shoulder flow zone material from the leading edge was confined in the weld cavity, and then a

sufficient amount of frictional heat and axial pressure was generated to produce a defect-free weld, Kumar and Kailas [5]. Accordingly, they concluded that deeper shoulder penetration leads to a decrease in the likelihood of welding defects. This conclusion is supported by the findings of Dubourg et al [13].

For tool number (3) welds perform excellent overall quality as illustrated in X-Ray Radiography as shown in fig.6.

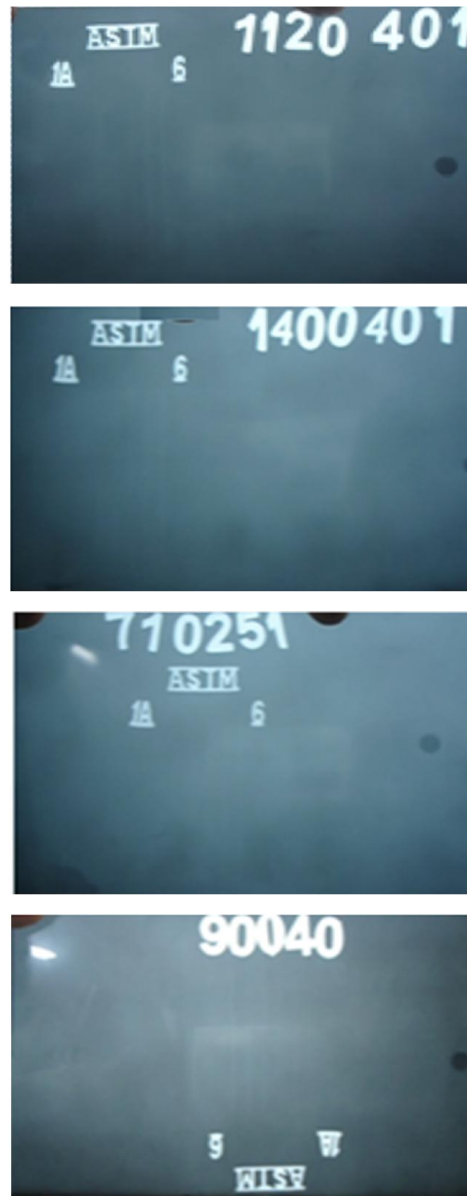


**Figure (6) X-Ray radiography inspection for tool (3) shows defect-free weld**

The inclination shoulder of tool (2) reduced to (2 degree), material flow in the shoulder flow zone is heavily affected by the tool shoulder inclination that gives enough time to flow from the zone under the shoulder to zone around the pin and in particular the shoulder forging function has the effect of locally increasing the deformation of the plasticized material as shown in fig 7.

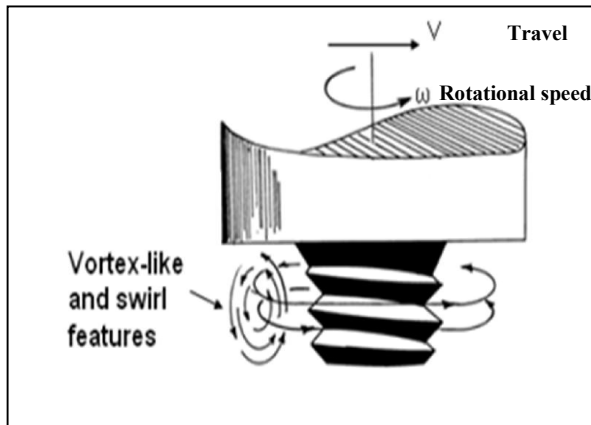


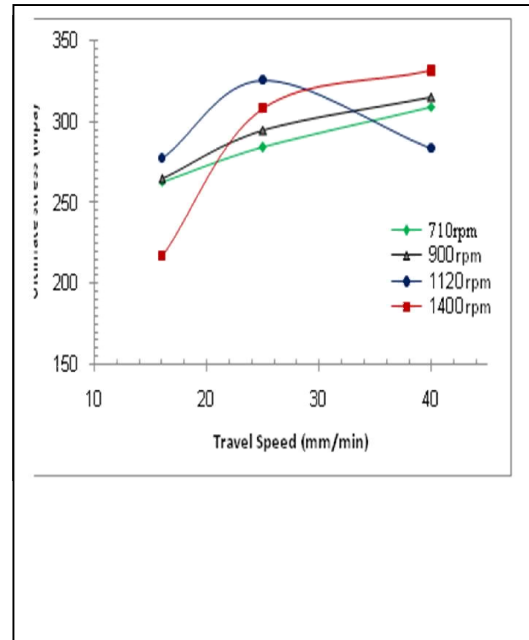
**Figure (7): Schematic illustration of the material flow has vortex-like and swirl features in the back of tool pin forming nugget zone [14]**

### Mechanical Property

The results of transverse tensile test are summarized in figures (8, 9 and 10). In general, both yield strength and ultimate tensile strength were reduced in the welded joints compared with that of the parent material, due to a combination of dissolution, coarsening and reprecipitate of strengthening precipitates during FSW or localized deformation.

Test result for first set of welding parameter (710rpm) with different welding speed (16,25 and 40mm/min) show that ultimate tensile strength have been increased with increasing welding speed . This investigation was repeated for other rotation speeds (710, 900, 1120 and 1400 rpm) .it is believed that the increasing in weld strength with

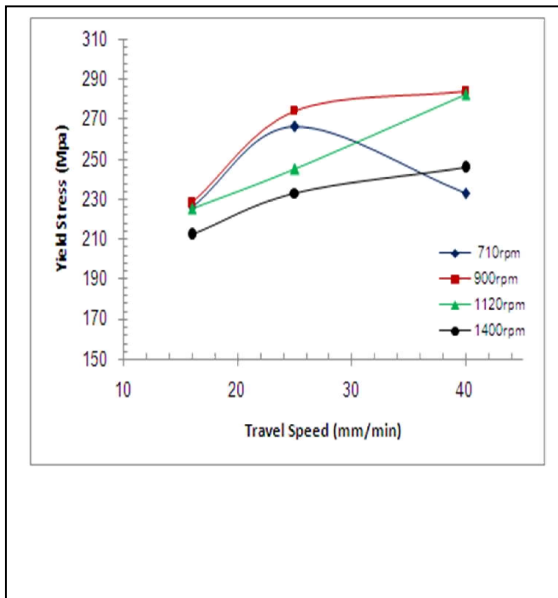
increasing welding speed was attributed to reduced heat input per unit length weld which resulted in less over aging of the weld zone From the result of FSW experiment performed in this paper compared with base metal the FSW joint exhibited reduced strength and ductility due to the overaged microstructure and localized deformation in the HAZ [15].



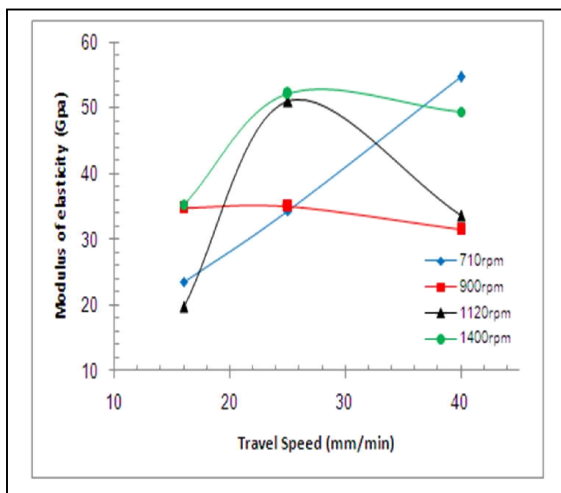
**Figure (8) Relationship between UTS and travel speeds at different rotational speeds**

Figure (8) shows the relationship between the UTS and rotational speeds at different travel speeds and figure (9) shows the relationship between the yield stress and the travel speeds at different rotational speeds. From the two figures it can be found that the optimum combination of rotation speed and travel speed was occurred at (1400 rpm) and (40 mm/min) that gives 83%welding efficiency for 5 mm thick AA7020-T53 aluminum alloy. The ultimate tensile strength increases with increase rotational speed and travel speed exert a

significant effect on the higher heat input and mechanical properties.



**Figure (9) Relationship between Yield stress and travel speeds at different rotational speeds**



**Figure (10) Relationship between modulus of elasticity and travel speeds at different rotational speeds**

From the shape and location of the tensile specimens fracture the following observations can be made. First, most of the FSW joints failed at heat affected zone (HAZ) on the advancing side. This

is consistent with other reports of FSW of aluminum alloys such as S. R. Ren et al. [16] and Sutton M. A. [17] Second, failure occurred in a plane nearly perpendicular to the tensile axis. Third, for the same travel speed, the variation in the rotation rate did not change the fracture mode and this conforms to investigation of Ren S. R. et al. [16] Fourth, near welding zone the fracture surface at parent material figure (11-a), which means that the welding parameters cause sufficient heat to fracture surface can be observed in specimens is that low elongation and welding efficiency have bright section figure (11-b) which means, that a sudden fracture occurred due to insufficient heat input during the FSW.

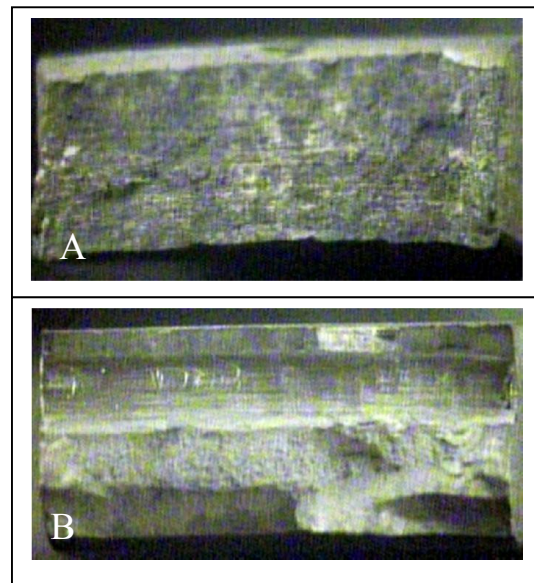


**Figure (11) Fracture surface of A) parent material (ductile fracture) and B) brittle fracture**

After the welded joints have been obtained each joint is subjected to the three point bending test using universal testing machine. this test is used for testing both base metal and welded joint

(fig.12-a,b,c and d)The results of bending test are conducted in accordance with the tensile test results, which means, that the best bending force values were achieved at (40 mm/min) travel speed for (900rpm) rotational speed. Fig.12-a shows bending test of the base metal fig.12-b and fig12-c shows increase of bending load with increase of travel speed, no cracking was observed in bend test of the joints in fig12b-d.

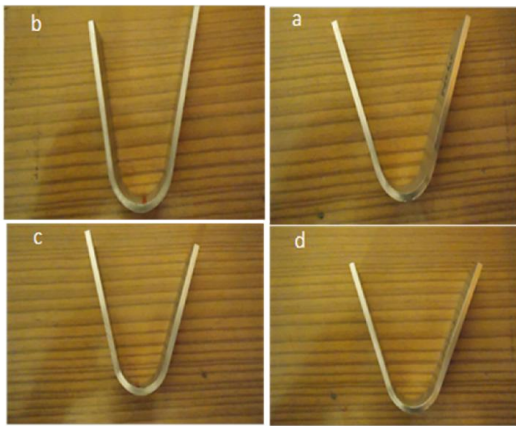


**Figure 12: bending test a: base metal (17.85kN) b: 900rpm-40mm/min (16.18kN) c: 710rpm-40mm/min (11.69kN) d: 1120rpm-25mm/min(13.27kN)**

**Microhardness distribution:**

The hardness measurements were performed with 1-mm spacing across the weld and location at 75mm in the welding path mid position of along welding line. Both horizontal profiles of Vickers hardness in the weld zones and parent metal are shown in Fig. (13), Welding parameters used 1400rpm (16mm/min&40mm/min) and (900rpm, 40mm/min). The variations in microhardness can be directly correlated to weld locations by overlaying the microhardness plot on the image of the weld section.

Microhardness results show that an increase in hardness values in nugget zone in (1400rpm,40mm/min) as compared with (1400rpm,16mm/min) increasing travel speed reduce thermal history and related to small grain size and dislocation density of the nugget zone .

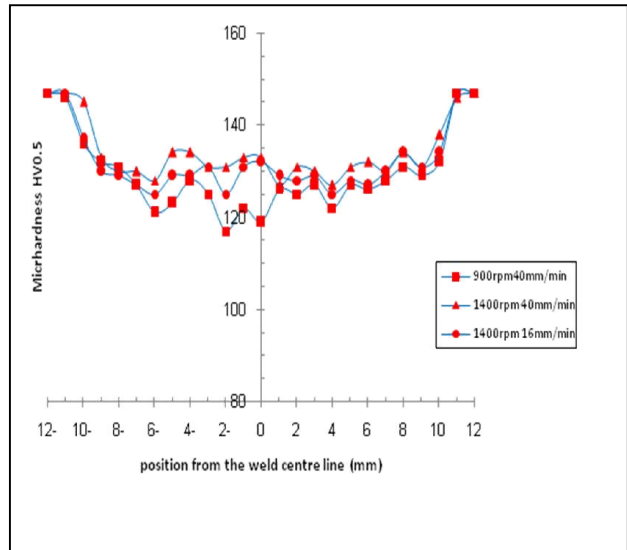


**Figure (13) Microhardness distribution of the welded zones with different rotation and travel speeds**

In general the microhardness values in all welding areas are reduced compared with that of the base metal (146 HV0.5), this means that the heat generated during FSW causes softening of the welded area due to grain coarsening or dissolution of precipitates and that conform to results of Terry Khaled [18], FSW temperatures arrival to the NZ and parts of the TMAZ, will cause at least partial dissolution of the hardening phases. Ordinarily, therefore, some softening within the NZ should be expected in heat treatable alloys that were welded in T-temper. Some graincoarsening and softening could also take place in the HAZ.

The decreasing in the weld hardness can be attributed to the dissolution of

precipitates and subsequently the weld cooling rates do not favor nucleation and growth of all precipitates [19].

From comparing the hardness distribution for two travel speeds it can be found that the FSW joint welded at high travel speed of 40 mm/min exhibited higher hardness values than that at the lower travel speed of 16 mm/min, which indicate that the thermal exposure experienced by the former is less than that experienced by the latter.

It can be seen from figure (13), that minimum hardness values are observed in both sides of the weld in the HAZ. Because of post weld thermal cycle the pre-precipitation is possible in the material where the precipitates are dissolved in matrix and the hardness can be recovered. But hardness cannot be recovered in the region where the precipitates grow. Re-appearing of precipitates in the NZ and TMAZ is cause for hardness recovery. In the HAZ precipitates are not dissolved in the matrix, and consequently there is no reappearance of precipitates due to post weld thermal cycle. This causes the lowest hardness and consequently fractures during tensile testing in the HAZ and that conform to Kumar K. [5]

Figure (14) shows the hardness distribution from bottom to top of the plate thickness at (1400rpm, 16mm/min), and (1400rpm, 40mm/min) and (900 rpm and 40 mm/min). From this figure, the hardness values decrease with decreasing travel speed because increased the thermal cycle for low travel speeds. While, the hardness values increase as a result of decreasing the heat input and fine grains and that conforms to results of Sutton M. A. et al. [17] and , the hardness increases as the rotation speed increases due to the

increase in heat input and dynamic plastic deformation increase.

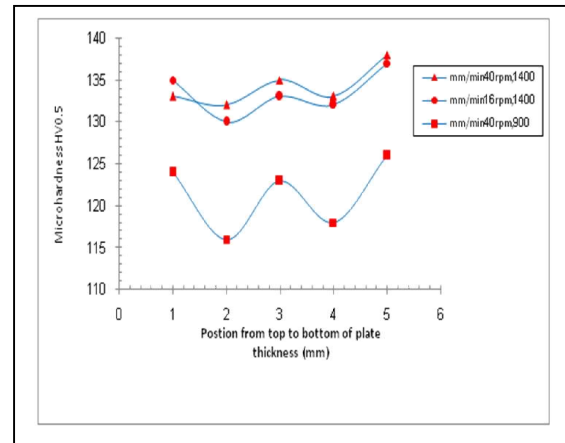


**Figure (14) Microhardness distribution along plate thickness**

#### Microstructure of welded area:

The microstructures of the welds are shown in Fig.15. It is clearly evident from those figures that the overall shapes of the nugget vary depending upon the process conditions. It is imperative to note that width of the weld is decreasing when the traverse speed is increased. This is due to the influence of lower heat input and plastic work that takes place at higher speed.

The contribution of intense plastic deformation and high temperature exposure within the stirred zone during FSW results in recrystallization and development of the texture within the stirred zone and precipitates dissolution and coarsening within and around the stirred zone [19].

Optical macroscopic examination was carried out on joints welded at 40 mm/min travel speed and different rotation speeds 900 and 1400 rpm as shown in fig.15, then the same examination was repeated on joints welded at 1400 rpm and different travel speeds 16 and 40 mm/min as shown in fig.15 Optical macroscopic revealed that

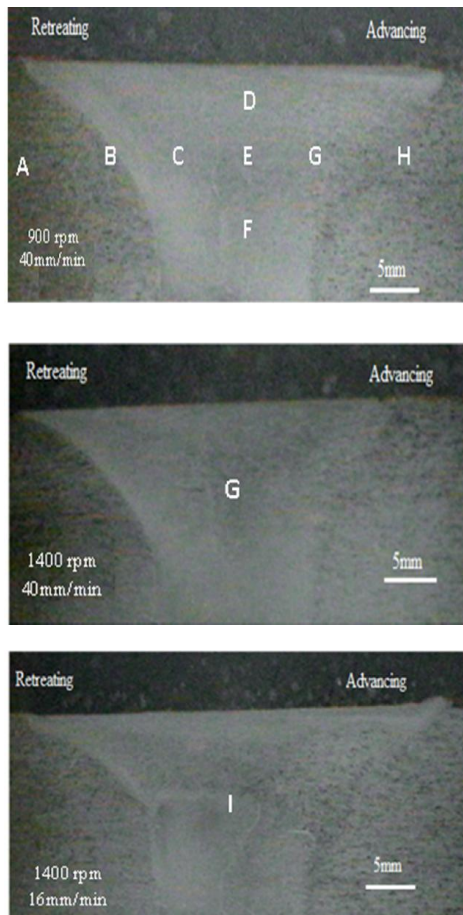


**Figure (15) Macrograph of FSW at different travel and rotational speeds**

no porosity or other defects (such as kissing bond) exist in the stirred zones of most joints produced except those welded at 16 mm/min travel speed (that conforms with tensile and bending tests results).

The microstructure of the parent material is shown in Fig. 16-A. It is often preferred to measure the grain size by lineal intercept technique [20]. It consists of elongated grain morphology (pancake shaped grains) having the size of 34  $\mu\text{m}$ . It has higher hardness due to strain-hardening effect by rolling. In FSW, three different microstructural zones are identified such as weld nugget, TMAZ, and unaffected base material. Weld

nugget has a recrystallized microstructure that consists of equiaxed grains as shown in Fig. 16-A. These grains are homogeneous at lower speed than the higher welding speed. It occurs because of sufficient heat input to form homogeneous grains. Grain size of the nugget is decreasing with the increase of weld traverse speed. Eventually, a grain size of 22.5  $\mu\text{m}$  is obtained at low traverse speed (16mm/min). Similarly, lower grain size of 20  $\mu\text{m}$  is also noted at higher travel speed (40mm/min) fig. (16-D), fig.(16-G) and fig.(16-I). Thermomechanically affected zone is characterized by rotation of the elongated grains of the parent metal as shown in Fig.(16-B) and fig.(16-H), The orientation of the grain along the rolling direction as in parent metal is absent, even though the grains are plastically deformed and thermally affected.

Next to the TMAZ is the HAZ which received no plastic deformation but has only been subjected to thermal exposure and therefore the original elongated grain structure of the base alloy is retained with an average grain size of (24 $\mu\text{m}$ ) for 900rpm and 40mm/min welding speed condition, although strengthening precipitates may overage and coarsen leading to degradation of mechanical properties of this region [21] which are connected to the location of fracture in tensile test and the lower hardness values were achieved in the HAZ.

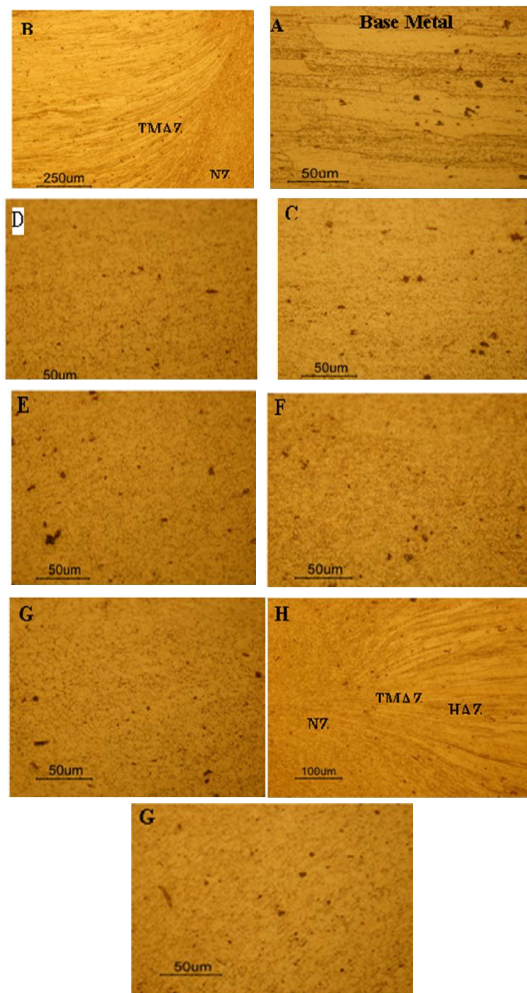


**Figure (16)** Microstructures of the weld nugget zone and TMAZ under the various welding conditions: (A) Base metal , (B) TMAZ in retreating side , (C) nugget zone in retreating side, (D) upper nugget zone (E) middle nugget zone, (F) lower nugget zone, (G) nugget zone in advance side, (H) middle nugget zone (1400rpm,40mm/min) and (I) middle nugget zone (1400rpm,16mm/min)

### Conclusion:

- In general, two defects were observed in FSW due to insufficient stirring of metal and higher and lower heat input. These are termed as continuous tunnel behind pin in advance side and tunnel under the pin above the root.

- Threaded cylinder pin has provided a good indication of material flow direction the highly deformed shear zone around the pin is characterized by the total disappearance of the original rolled structure of the work piece material.
- Increasing inclination of shoulder surface increasing the time required to flow material behind pin and compressed by shoulder surface.
- Hardness for base metal is higher than welded joints and increases with increasing travel speed and rotational speed.
- Grain size for base metal is higher than welded joints and decreases with increase travel speed and rotational speed. FSW process gives fine and equiaxed grains in the middle nugget zone  $22.5\mu\text{m}$  and  $20\mu\text{m}$  at travel speed  $16\text{mm}/\text{min}$  and  $40\text{mm}/\text{min}$  respectively as compared with grains of the parent metal  $34\mu\text{m}$  while they are  $24\mu\text{m}$  in the  $40\text{mm}/\text{min}$  with  $900\text{rpm}$ .
- FSW optimal conditions for a 5-mm thick plate of aluminum alloy AA7020-T53, which produce 83% welding efficiency, are 1400 rpm rotation speed and 40 mm/min travel speed.
- The fracture of the tensile test specimens welded by FSW occurred in the HAZ region.
- Hardness increases with increasing rotational speed and decreases with increasing travel speed.
- Grain size of the nugget zone is decreasing with the increase of welding traverse speed.

**References:**

1. Liu HJ, Fujii H, Maeda M, Nogi K (2003) "Tensile properties and fracture locations of friction-stir-welded joints of 2017-T351 aluminum alloy". *J Mater Process Technol* 142: pp.692–696 doi: 10.1016/S0924-0136(03)00806-9.
2. Peel M, Steuwer A, Preuss M, Withers PJ (2003) "Microstructure, mechanical properties and residual stresses as a function of welding speed in aluminum AA5083 friction stir welds". *Acta Mater* 51:4791–4801 doi:10.1016/S pp.1359-6454(03)00319-7.
3. AbbasiGharacheh M, Kokabi AH, Daneshi GH, Shalchi B, Sarrafi R (2006) "The influence of the ratio of "rotational speed/ traverse speed" (w/v) on mechanical properties of AZ31 friction stir welds". *Int. J. Mach. Tool.Manufact.* 46: pp.1983–1987.
4. Venugopal T, SrinivasaRao K, Prasad Rao K (2004) "Studies on friction stir welded AA 7075 aluminium alloy". *Trans Indian InstMetab* 57(6): pp.659–663.
5. Kumar K, SatishV.Kailas." on the role of axial load and the effect of interface position on the tensile strength of a friction stir welded aluminum alloy".*Materials and Design* 29 (2008) pp.791-797.
6. Gaafer A.M., Mahmoud T.S., Mansour E.H." Microstructural and mechanical characteristics of 7020-0 Al plates joined by friction stir welding" *Material science and engineering A527* (2010) pp.7424-7429.
7. Z.W.Chen, T Pasang, Y. Qi. "Shear flow and deformation of nugget zone during friction stir welding of aluminum alloy 5083-0" *material science and engineering A* 474(2008) pp.312-316.
8. M. Awing,I.M. Ahmat and P. Hussain "Experience on friction stir welding and friction stir spot welding at universiti teknologi etronas" *journal of applied sciences* 11(11): pp.1959-1965, 2011.
9. H.B. Chen, K. Yan, T. Lin, S.B. Chen, C.Y. Jiang, Y. Zhao, *Mater. Sci. Eng.A* 433 (2006) pp.64–69.
10. Leal R, Loureiro A. "Defects formation in friction stir welding of aluminum alloys" *Mater. Sci. Forum* 2004; 455-6: pp.299-302.
11. K. Elangovan, V. Balasubramanian "Influences of tool pin profile and tool shoulder diameter on the formation of friction stir processing zone in AA6061 aluminium alloy" *Materials and Design* 29 (2008) pp.362–373.
12. Fuller, C.B., *Friction stir tooling: tool materials and designs*, in *Friction stir welding and processing*, R.S. Mishra and M.W. Mahoney, Editors. 2007, ASM International: Materials Park, OH. pp. 14-15.
13. Dubourg, L., et al., *Process window optimization for FSW of thin and thick sheet Al alloys using statistical methods*, in *6th International FSW Symposium*. 2006: Montreal, Canada.
14. Prado, R.A., et al., *Self-optimization in tool wear for friction-stir welding of Al 6061+20% Al<sub>2</sub>O<sub>3</sub> MMC*. *Materials Science and Engineering A*, 2003. 349(1-2): pp.156-165.
15. Kevin J. Colligan et al. "friction stir welding demonstrated for vehicle construction. *American welding society.Welding journal*, 51 (2004) pp.243–248.
16. Ren S. R., Ma Z. Y. and Chen L. Q., "Effect of welding parameters on tensile properties and fracture behavior of friction stir welded Al-Mg-Si alloy", *ScriptaMaterialia*, Vol, 56, October 2006, pp. 69-72.
17. Sutton M. A., Yang B., Reynolds A. P. and Taylor R., "Microstructural studies of friction stir welds in 2024-T3

aluminum", Materials Science and Engineering A323, March 2001, pp. 160-166.

18. Terry Khaled, "An Outsider Looks at Friction Stir Welding" ANM-112N-05-06 (July 2005).

19. Venugopal T., Roa K. S. and Roa P., " Studies on friction stir welded A7075-T6 aluminum alloy", Trans. Indian Inst. Met., Vol. 57, No. 6, December 2004, pp. 659-663.

20. Meyers M. A., Chawla K. K., "Mechanical behavior of materials", Prentice-Hall, Inc., USA, 1999.

21. Mohamedtahir M. SaeedMulapeerZibary, "Metallurgical and Mechanical Properties of Some Friction Stir Welded Aluminum Alloys", PhD Thesis, University of Salahaddin-Erbil, 2009.

## تأثير الشكل الهندسي لاداة اللحام على النوعية والخصائص الميكانيكية للملحومات بطريقة الخلط الاحتكاك لسبيكة الالمنيوم (7020-T53)

محمد عبدالستار محمد

جامعة النهريين - كلية الهندسة

منير حميد ظليفيح

هيئة التعليم التقني

الكلية التقنية بغداد

محسن جبر جويج

جامعة النهريين - كلية الهندسة

### الخلاصة:

في هذا البحث تم دراسة تأثير تغيير الابعاد الهندسية لعدة اللحام وعناصر اللحام (السرعة الخطية و السرعة الدورانية) على نوعية اللحام والخواص الميكانيكية لسبيكة المنيوم (7020-T53) باستخدام اللحام بالخلط والاحتكاك.

تم استخدام ثلاث متغيرات لاداة اللحام (الكتف, انحناء الكتف والعمود) حيث ان نفق داخلي (tunnel) اكتشف من خلال الفحص الشعاعي و لجميع متغيرات اللحام ( السرعة الخطية و الدورانية) ووجد أن أفضل ابعاد أعطت لحام خالي من العيوب كانت (بزيادة قطر رأس أداة اللحام العمود مع التسنين و زيادة قطر الكتف مع أفضل انحناء لسطح الكتف كان (2°) وتم التأكد من خلوص وصلات اللحام من العيوب باستخدام الفحص الشعاعي حيث ان زيادة الابعاد و التسنين تؤدي الى زيادة عملية الخلط وكمية الحرارة المتولدة.

تأثير متغيرات اللحام (السرعة الدورانية و الخطية) باستخدام الشكل الهندسي لأداة اللحام الذي أعطى وصلات لحام خالية من العيوب تم دراستها بالاعتماد على الفحوصات الميكانيكية الاتلافية ( فحص الشد, فحص الانحناء, فحص الصلادة المايكروية و البنية المجهرية).

بناء على التجارب اعلاه تم الحصول على اقصى كفاءة لحام وصلت الى ( 83% ) اعتمادا على مقاومة الشد باستخدام متغيرات اللحام المثلى (40mm/min, 1400rpm). كما تبين ان زيادة السرعة الدورانية يؤدي الى زيادة الصلادة المايكروية في منطقة اللحام بينما تؤدي الى تقليل الحجم الحبيبي .